QUANTITATIVE THREE-DIMENSIONAL RECONSTRUCTION OF LIMITED-ANGLE EXPERIMENTAL MEASUREMENTS IN DIFFRACTION TOMOGRAPHY

Chen-Hao Chang[⋆] *Jing-Wei Su*[†] *Wei-Chen Hsu*[†] *Kung-Bin Sung*[†] *Cheng-Ying Chou*[⋆]

[⋆]Department of Bio-Industrial Mechatronics Engineering, National Taiwan University, Taipei, Taiwan
[†]Graduate Institute of Biomedical Electronics and Bioinformatics, National Taiwan University, Taipei, Taiwan

ABSTRACT

Image reconstruction from limited-angle data is an important issue in diffraction tomography. The limitation of angular coverage usually occurs due to the physical constraints in measurement systems. Insufficient information will deteriorate the quality of reconstructed images. In our experimental setup, the angular range of the data scanning is limited. Here, we applied the iterative algorithm of total variation (TV) minimization to reconstruct the three-dimensional distribution of an object's refractive index from measured phase data. TV-minimization is an edge-preserving technique commonly used in image processing. It can smooth away the noisy textures while retaining sharp edges. Despite a full range of illumination is lacking, we have successfully reconstructed the refractive index distribution of objects numerically and experimentally by use of the TV-minimization algorithm.

Index Terms— Diffraction tomography, image reconstruction, limited-angle, TV-minimization, edge-preserving

1. INTRODUCTION

Diffraction tomography (DT) is an image technique that explores the wave property of electromagnetic wavefield and aims to produce the object's refractive index distribution. X-ray computed tomography (CT) can be viewed as a limiting case of DT. Unlike CT that uses X-ray as the incident source, DT is suitable for acoustic waves or electromagnetic waves with longer wavelengths. The principle of diffraction tomography is described by Fourier diffraction theorem, which was first proposed by Wolf in 1969 [1]. He demonstrated that the three-dimensional (3D) structure of weakly scattering objects can be reconstructed from multiple two-dimensional (2D) scattered field measurements.

Based on the Fourier diffraction theorem, the reconstruction methods in DT can be divided into two main categories of analytic and iterative methods. Filtered-backpropagation (FBPP) [2] and Fourier mapping are the most widely used analytic solutions in DT. FBPP algorithm is generally considered more accurate than Fourier mapping. However, FBPP algorithm is much more time-consuming than Fourier mapping [3]. Therefore, the Fourier mapping method is adopted more than FBPP due to its low computational cost.

The data truncation can significantly affect the results of reconstruction. Therefore, an image reconstruction method that can mitigate such adverse effects and improve the reconstructed image quality is of great importance in practical applications. Sung et al. applied an iterative constraint method to reduce the effects of missing projections to obtain a quantitative 3D mapping of refractive index in live biological cells [4]. The positivity constraint in the iterative constraint method helps the reconstructed image recover its edge. However, the images they obtained show a strong oscillation across the central line of the object [5]. LaRoque et al. applied TV-minimization algorithm to obtain accurate 2D image reconstruction from few-view and limited-angle data [6] using simulated data.

In our preliminary study, the concept of limited-angle DT reconstruction was applied to simple latex spheres to demonstrate the efficacy of this method in real data application. Subsequently, we will extend our studies to tissue imaging to investigate the usefulness and limitation of DT under limited-angle conditions.

2. METHODS

In this work, we used (i) the Fourier mapping method to reconstruct the refractive index distribution of 3D objects, and (ii) applied TV-minimization algorithm with positivity constraint to improve the quality of reconstructed images.

2.1. Imaging physics of diffraction tomography

Consider that a monochromatic plane wave propagates along the z_r-axis and irradiates on an object. The rotated coordinate is related to the reference coordinates as $z_r = z\cos\theta + x\sin\theta$, with θ denoting the tomographic view angle measured from positive y-axis. The incident wavefield can be written as $u_0(\vec{r}) = e^{j\phi}$, where ϕ is the phase of the wavefield. The characteristics of the object can be represented by its scattering

This work was supported in part by National Science Council under grant No. NSC99-2221-E-002-043-MY3. Send correspondence to chengying@ntu.edu.tw.

potential $f(\vec{r})$,

$$f(\vec{r}) = k_0^2 \left[n(\vec{r})^2 - n_0^2 \right], \tag{1}$$

where $k_0 = 2\pi/\lambda$ is the wavenumber of the medium; λ is the wavelength of the incident wave; $n(\vec{r})$ and n_0 are the complex refractive index of the object and medium, respectively.

According to Fourier diffraction theorem [1], the Fourier transform of the scattered field of an object yields its Fourier transform over a semicircular arc when illuminated by a plane wave. In other words, the 3D Fourier transform of the object's scattering potential can be obtained from the scattered field detected at different angles.

2.2. Imaging system

In our measurement system, the phase measurements are acquired by rotating the light source while keeping the detector and object fixed (Fig. 1). Similar to the derivation in Ref. [1], the formulations for our measurement system are given by

$$\tilde{F}(K_x, K_y, K_z) = \frac{j\omega}{\pi} e^{-j\omega z} \tilde{U}_s(k_x, k_y), \tag{2}$$

where the angular frequency components k_x and k_y of the detector are related to the frequency components of the scattering potential as

$$\begin{cases} K_x = k_x - k_0 \sin\theta \\ K_y = k_y \\ K_z = \omega - k_0 \cos\theta, \end{cases} \tag{3}$$

and $\omega = \sqrt{(n_0 k_0)^2 - k_x^2 - k_y^2}$. Here, $\tilde{F}$ and $\tilde{U}_s$ are the 3D and 2D Fourier transforms of the scattering potential $f(\vec{r})$ and the detected scattered field $u_s(\vec{r})$, respectively. Here, we assume the incident plane wave is homogeneous and therefore, $k_x^2 + k_y^2 \leq k_0^2$ [1].

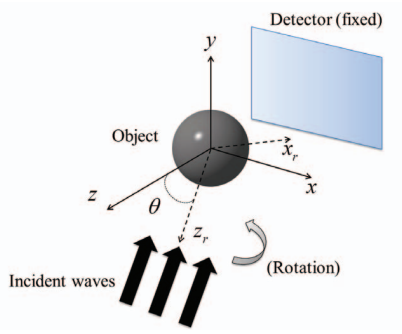


Fig. 1. The imaging geometry of the measurement system. The light source rotates whereas the detector and the object are fixed.

After collecting phase images $\phi_s(\vec{r})$ at different angles, we applied Eq. (2) to get the 3D Fourier transform of the scattering potential along semicircular arcs $\tilde{F}(K_x, K_y, K_z)$. Since the phase shift of the incident field in our measurement system is larger than π, we can use the measured phase $\phi_s(\vec{r})$ to estimate the scattered field $u_B(\vec{r})$ in a simple relationship [7]

$$\phi_s(\vec{r}) = \frac{u_B(\vec{r})}{u_0(\vec{r})}, \tag{4}$$

where $u_B(\vec{r})$ is the scattered field estimated by the Born approximation. Here, we assume the incident wave $u_0(\vec{r}) = 1$. By the Fourier mapping method, the scattered field $f(\vec{r})$ can be obtained directly from taking the inverse Fourier transform of this frequency distribution, $\tilde{F}(K_x, K_y, K_z)$, which is mapped into uniform grids through interpolation.

2.3. TV-minimization algorithm

The iterative reconstruction algorithm we applied is divided into two main parts: (i) data consistency step and (ii) TV minimization step. The objective of the data consistency step is to ensure that the L_2 norm between the estimated data and measured data is smaller than the tolerance value, namely $\left| \tilde{F} - \tilde{F}_0 \right| \leq \epsilon$. $\tilde{F}$ and $\tilde{F}_0$ correspond to the discrete Fourier transform (DFT) of the current estimated and measured data, respectively. ϵ is the tolerance chosen according to the noise level. In the TV-minimization step, the steepest descent algorithm was applied to yield a solution that satisfies

$$f^* = \arg\min \left\| \vec{f} \right\|_{TV} \text{ such that } \left| \tilde{F} - \tilde{F}_0 \right| \leq \epsilon. \tag{5}$$

In the data consistency step, we employed projection onto convex sets (POCS) by copying a fraction of the frequency information of measured data into the estimated data to maintain the data consistency (Eq. (6)), i.e.,

$$(1 - \beta) \cdot \tilde{F} + \beta \cdot \tilde{F}_0, \tag{6}$$

where β is the relaxation parameter decreasing steadily along with the iterative process from 1 to 0 [6]. Before doing the POCS step, we set the missing projections to zero value. Then, the Fourier mapping method was applied to fill the current data into the 3D frequency domain. Here, the initial guess image is set as a zero matrix. Followed by the application of inverse DFT, an intermediate image is obtained. Next, the positivity constraint was applied to ensure that the reconstructed refractive index is not smaller than that of the medium, i.e.,

$$f_{i,j,k} \geq 0 \quad \forall i, j, k, \tag{7}$$

where i, j, k are integer-valued indices of the scattering potential in the discrete form $f_{i,j,k}$.

The purpose of the steepest descent algorithm is to implement the TV minimization. In the field of image processing, the edge-preserving technique is to restore the destroyed image. It has the advantage of denoising and deblurring without

smearing sharp edges [9]. TV-minimization is a kind of methods used for edge-preserving. It has been applied in diffraction tomography for 2D simulation to obtain accurate image reconstruction of numerical results [6]. Here, the TV of an 3D object is defined as

$$\left\|\vec{f}\right\|_{TV} = \int |\nabla f|\, dxdydz = \int \sqrt{f_x^2 + f_y^2 + f_z^2}\ \ dxdydz, \tag{8}$$

where ∇f is the gradient of the image and f_x, f_y and f_z represent the partial derivative in each dimension; namely, $f_x = \partial f/\partial x$, $f_y = \partial f/\partial y$, and $f_z = \partial f/\partial z$. Interested readers can refer to Ref. [11] for the discrete form of $\partial\|\vec{f}\|_{TV}/\partial f_{i,j,k}$. The details of the TV-minimization algorithm is described in Ref. [10].

Each iteration alternately enforce the data consistency and TV-minimization steps till the stopping criteria is met.

3. NUMERICAL STUDIES

In numerical studies, we applied the TV-minimization algorithm with positivity constraint to reconstruct the refractive index distribution of an tissue-like object. The object space is discretized to a $128 \times 128 \times 128$ matrix. The detector is set to cover from -60° to 60°, and the total number of scan is 180 views. The reconstruction results are displayed in Fig. 2. The underestimation inside the reconstructed object (Fig. 2(b)) by the Fourier mapping method is caused by insufficient low-frequency data. From the reconstructed results (Fig. 2(d)), the image quality has improved due to the application of the TV-minimization algorithm with positivity constraint. It means this method can successfully reconstruct the 3D objects from virtual data under limited-angle situations.

4. EXPERIMENTAL STUDIES

In this section, we applied the TV-minimization algorithm with positivity constraint to reconstruct a 10 μm polystyrene bead from experimental data.

4.1. Experimental setting

The measurement system is one kind of the tomographic phase microscopy. A 10 μm polystyrene bead (n= 1.6210) was immersed in oil (n = 1.5899). The wavelength of light source is 404.7 nm. The laser beam was rotated to cover from $-64^\circ \sim 64^\circ$ with the detector fixed. 789 phase images were acquired. Therefore, this can be seen as the limited-angle case. The magnification is 140X, and detector is an 512×512 array with the linear dimension of each detector element equal to 12 μm.

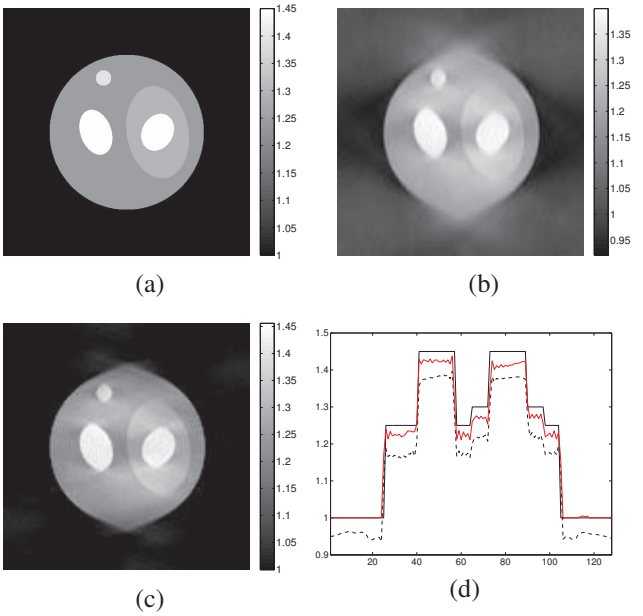


Fig. 2. (a) A slice of the tissue-like object's phantom at the plane $z = 0$, and the reconstructed results by use of (b) the Fourier mapping method, and (c) TV-minimization algorithm with positivity constraint. (d) The profile along x-axis at $y = 0$ and $z = 0$. The solid, dashed and red curves represent the phantom, the images obtained by use of the Fourier mapping and TV-minimization algorithm, respectively.

4.2. Experimental results

Fig. 3 shows the phase image of the polystyrene bead measured at zero degree illumination. We have applied the TV-minimization algorithm with positivity constraint to reconstruct the refractive index map of a three-dimensional polystyrene bead. The diameter of the bead is 10 μm. The refractive index of the bead and medium are respectively 1.6210 and 1.5899 at 404.7 nm wavelength.

The measured data were used to reconstruct an image volume of $512 \times 512 \times 512$ voxels. The reconstruction results are displayed in Fig. 4. In the image reconstructed using Fourier mapping method, the refractive value of the bead is underestimated (Fig. 4(b)). The underestimation is caused by incomplete angular data, which leads to the insufficient data in the frequency domain. After applying the TV-minimization algorithm with positivity constraint (Fig. 4(c)), the result was improved and shows closer resemblance to the true value. The improvement provided by use of TV-minimization algorithm can be seen by comparing Figs. 4(b) and 4(c).

5. CONCLUSION

Previously, TV-minimization algorithm has been applied to 2D diffraction tomography in numerical studies. In this

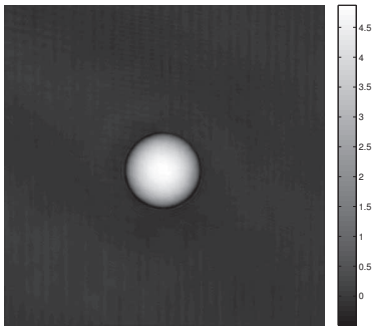


Fig. 3. Quantitative phase image of a 10 μm polystyrene bead taken at zero degree illumination. The color bar indicates the values of phase in radians.

research, we applied the TV-minimization algorithm with positivity constraint to reconstruct the 3D refractive index map of polystyrene bead from experimental data. Besides, this algorithm is tested to reconstruct ellipsoids from virtual data. The positivity constraint in the iterative process can make the index outside the bead larger than or equal to that of the medium. Reducing the TV of the image can recover the edge and preserve the information inside the object. The results prove that this algorithm can be applied successfully to polystyrene beads from experimental data and tissue-like objects in numerical simulation. The reconstruction of biological cells is not included in this research, and this is an important area to study in the future.

6. REFERENCES

[1] E. Wolf, "Three-dimensional structure determination of semi-transparent objects from holographic data," *Optics Communications*, vol. 1, no. 4, pp. 153–156, 1969.

[2] AJ Devaney, "A filtered backpropagation algorithm for diffraction tomography," *Ultrasonic imaging*, vol. 4, no. 4, pp. 336–350, 1982.

[3] S. Pan and A. Kak, "A computational study of reconstruction algorithms for diffraction tomography: interpolation versus filtered-backpropagation," *Acoustics, Speech and Signal Processing, IEEE Transactions on*, vol. 31, no. 5, pp. 1262–1275, 1983.

[4] Y. Sung, W. Choi, C. Fang-Yen, K. Badizadegan, R.R. Dasari, and M.S. Feld, "Optical diffraction tomography for high resolution live cell imaging," *Optics express*, vol. 17, no. 1, pp. 266–277, 2009.

[5] Y. Sung and R.R. Dasari, "Deterministic regularization of three-dimensional optical diffraction tomography," *JOSA A*, vol. 28, no. 8, pp. 1554–1561, 2011.

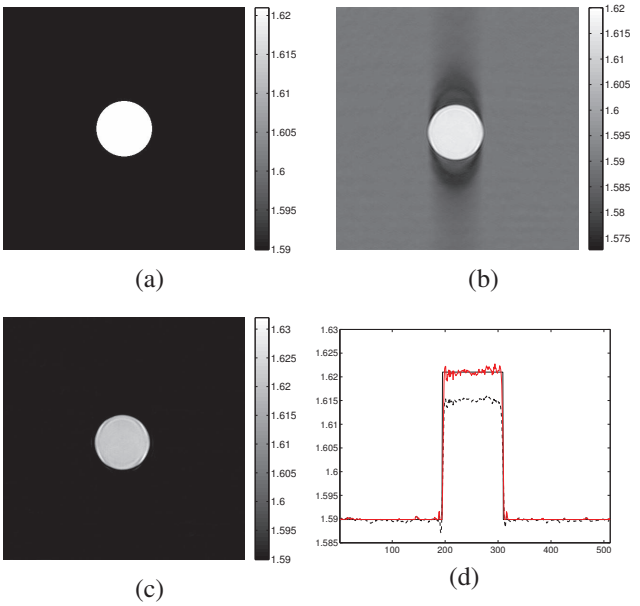


Fig. 4. (a) A slice of a 10 μm latex bead at $z = 0$, and those reconstructed by use of (b) the Fourier mapping method, and (c) TV-minimization algorithm with positivity constraint. (d) The profile along x-axis at $y = 0$ and $z = 0$. The solid, dashed and red curves represent the true phantom, the images obtained by use of the Fourier mapping and TV-minimization algorithm, respectively.

[6] S.J. LaRoque, E.Y. Sidky, and X. Pan, "Accurate image reconstruction from few-view and limited-angle data in diffraction tomography," *JOSA A*, vol. 25, no. 7, pp. 1772–1782, 2008.

[7] A.C. Kak and M. Slaney, "Principles of computerized tomographic imaging," 1988.

[8] W. Choi, C. Fang-Yen, K. Badizadegan, S. Oh, N. Lue, R.R. Dasari, and M.S. Feld, "Tomographic phase microscopy," *Nature methods*, vol. 4, no. 9, pp. 717–719, 2007.

[9] J. Yang, W. Yin, Y. Zhang, and Y. Wang, "A fast algorithm for edge-preserving variational multichannel image restoration," *SIAM Journal on Imaging Sciences*, vol. 2, no. 2, pp. 569–592, 2009.

[10] E.Y. Sidky and X. Pan, "Image reconstruction in circular cone-beam computed tomography by constrained, total-variation minimization," *Physics in medicine and biology*, vol. 53, pp. 4777, 2008.

[11] M. Persson, D. Bone, and H. Elmqvist, "Total variation norm for three-dimensional iterative reconstruction in limited view angle tomography," *Physics in medicine and biology*, vol. 46, pp. 853, 2001.